

Figure 1: General structure of activators of non-genomic Estrogen-Like Signalling (ANGELS).

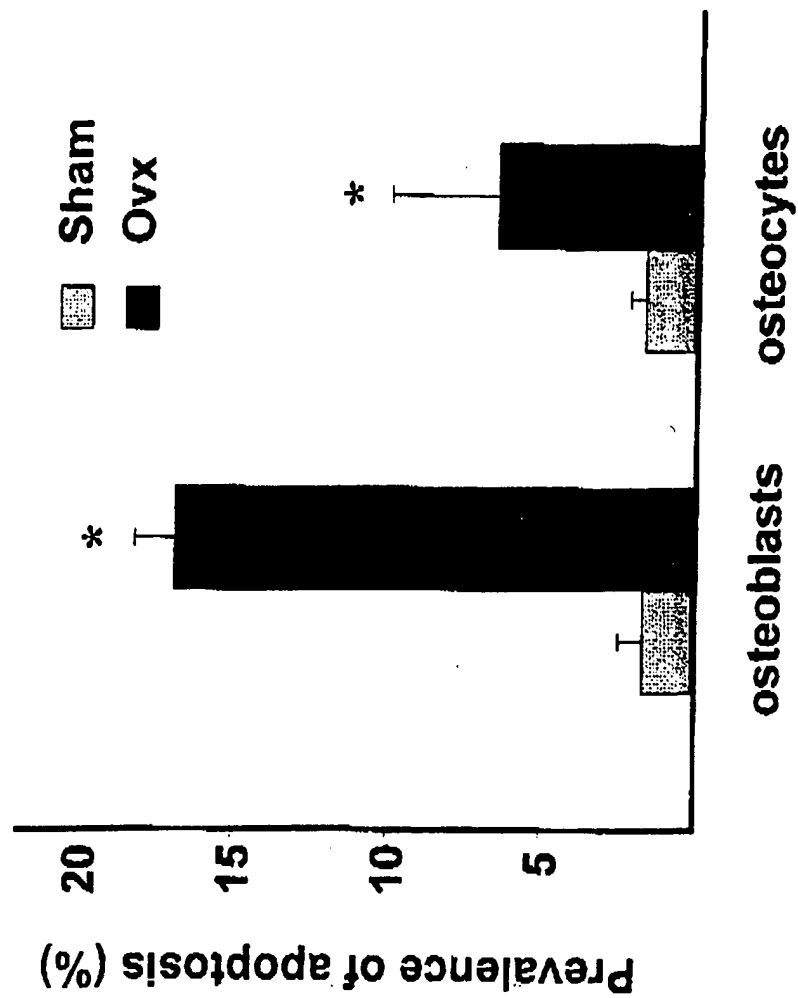


Figure 2: Estrogen deficiency causes increased apoptosis of osteoblasts and osteocytes in murine vertebral bone .

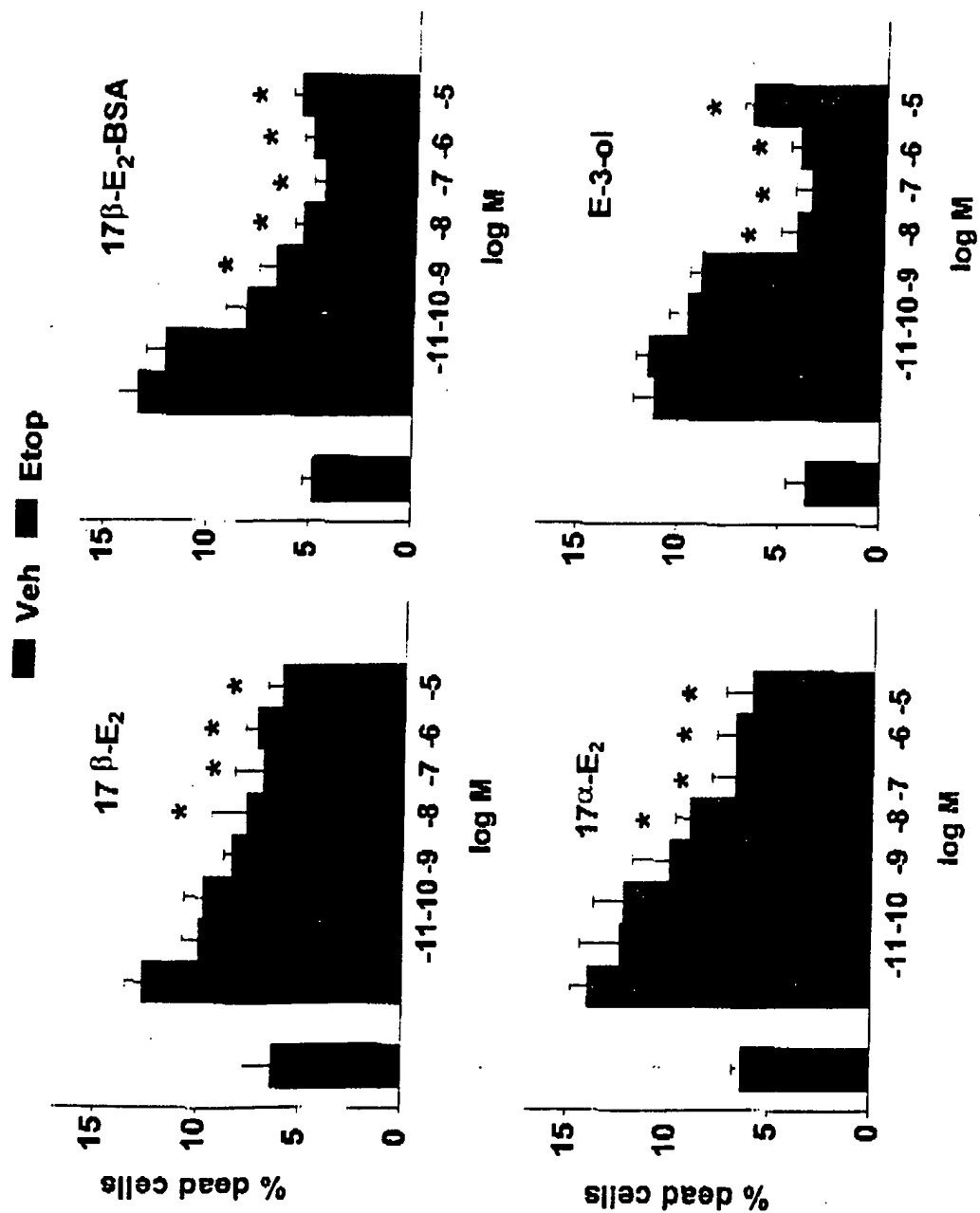


Figure 3: Inhibition of apoptosis of osteoblastic cells.

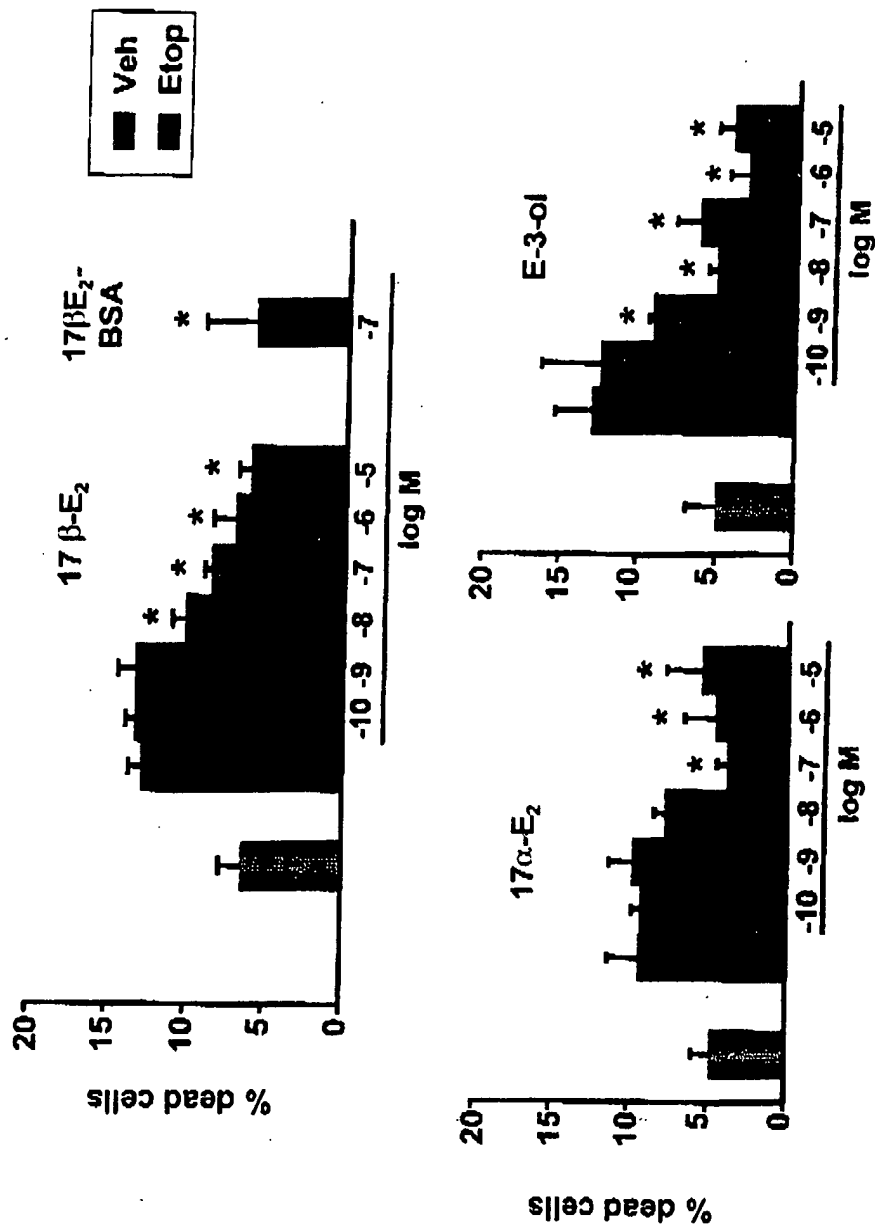


Figure 4: Inhibition of apoptosis of MLO-Y4 osteocytic cells by ANGELS

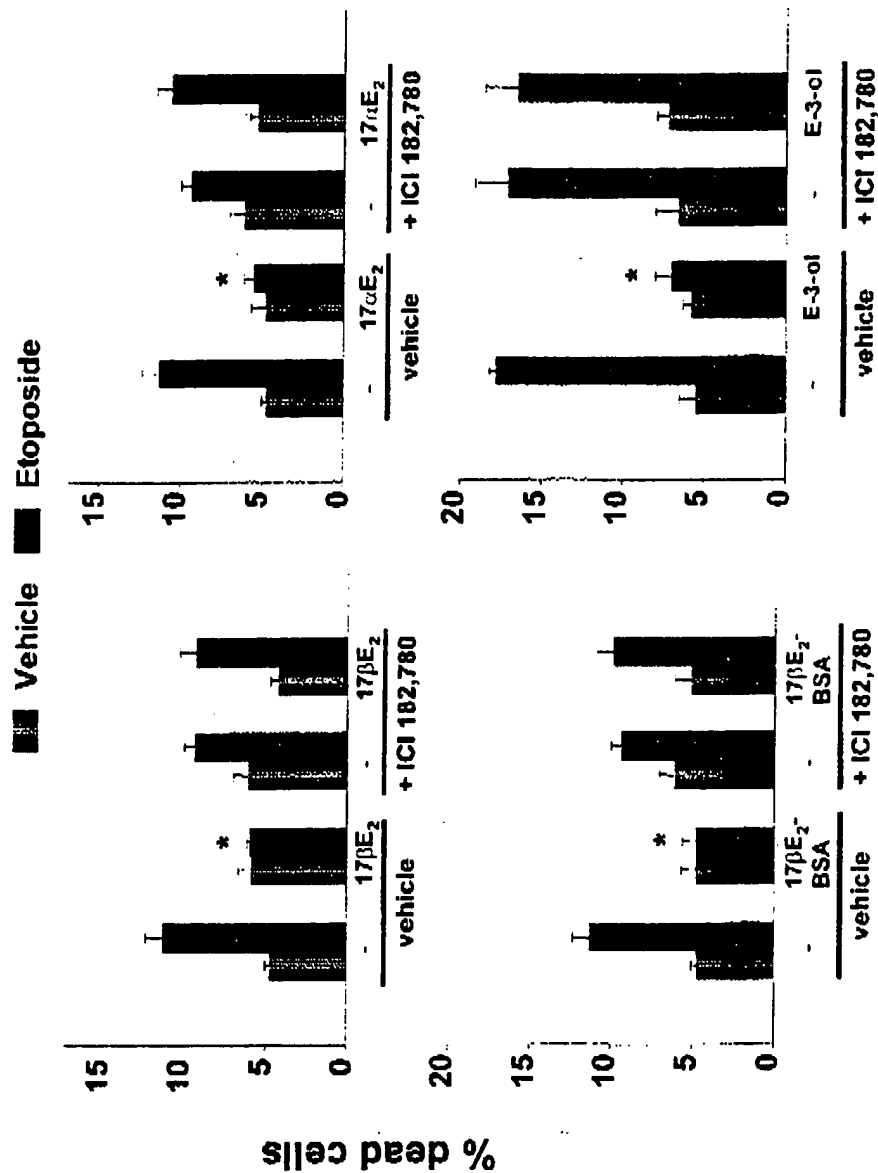


Figure 5: Blockade of the anti-apoptotic effect of estrogen and ANGELS by ICI 182,780 in osteoblastic cells

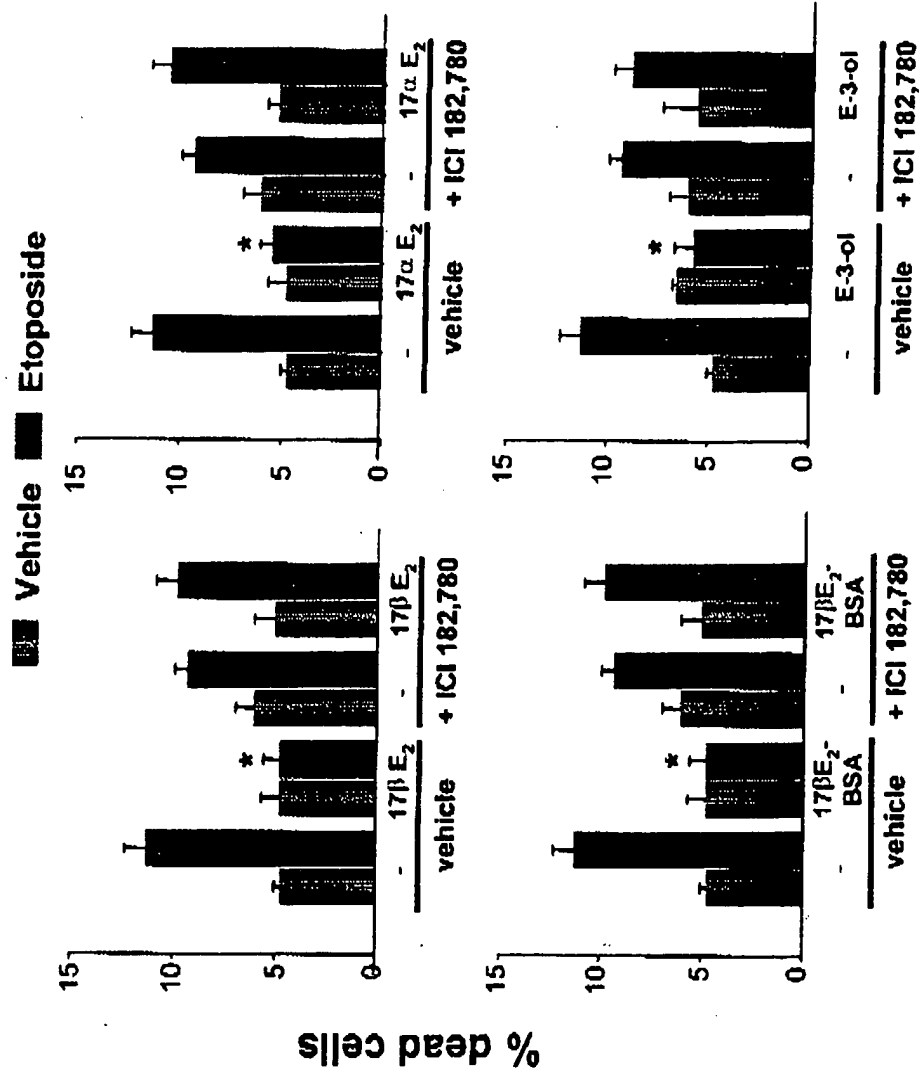


Figure 6: Inhibition of the antiapoptotic effect of estrogen and ANGELS by ICI 182,780 in MLO-Y4 osteocytic cells

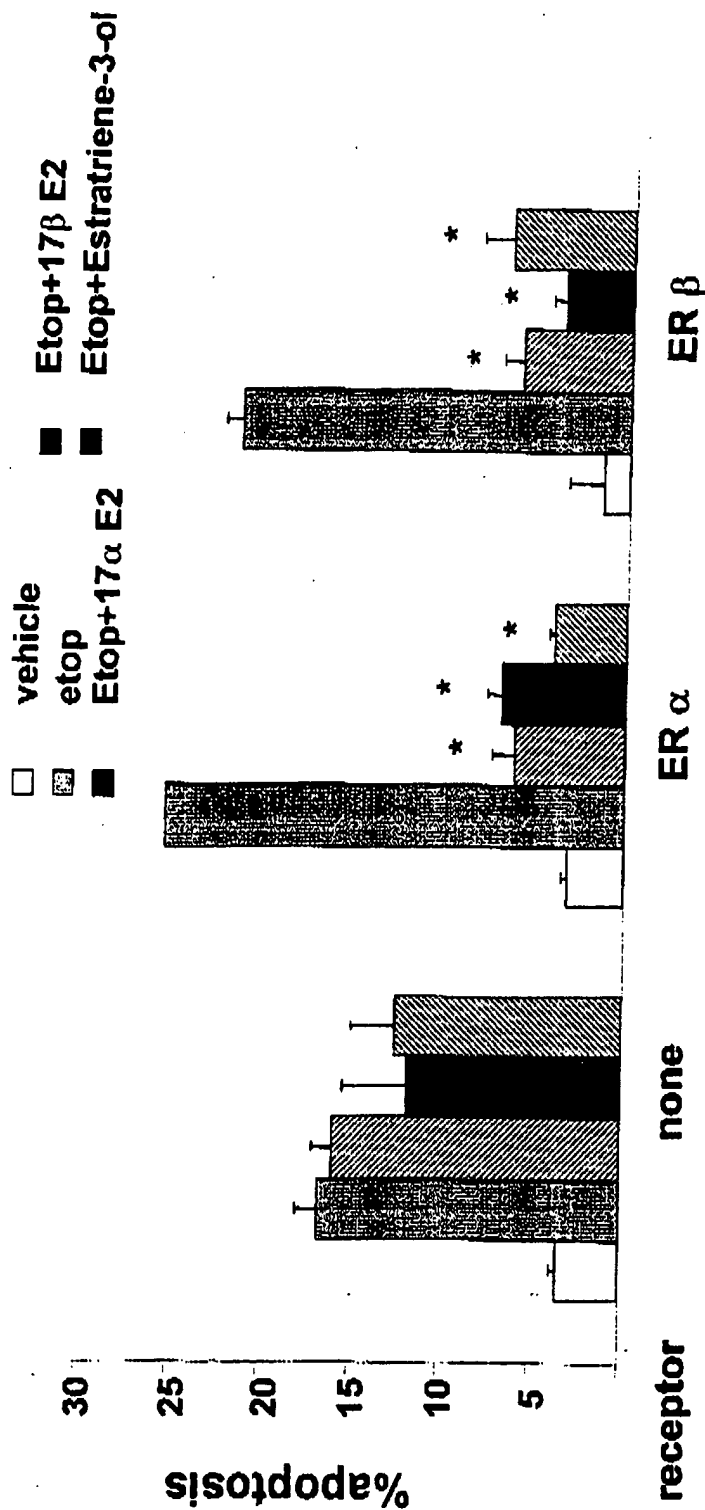


Figure 7: Estrogen receptor a or b is required for the antiapoptotic effects of 17b estradiol, 17a estradiol, and estratriene-3-ol on etoposide-induced apoptosis (experiment 1/21/99).

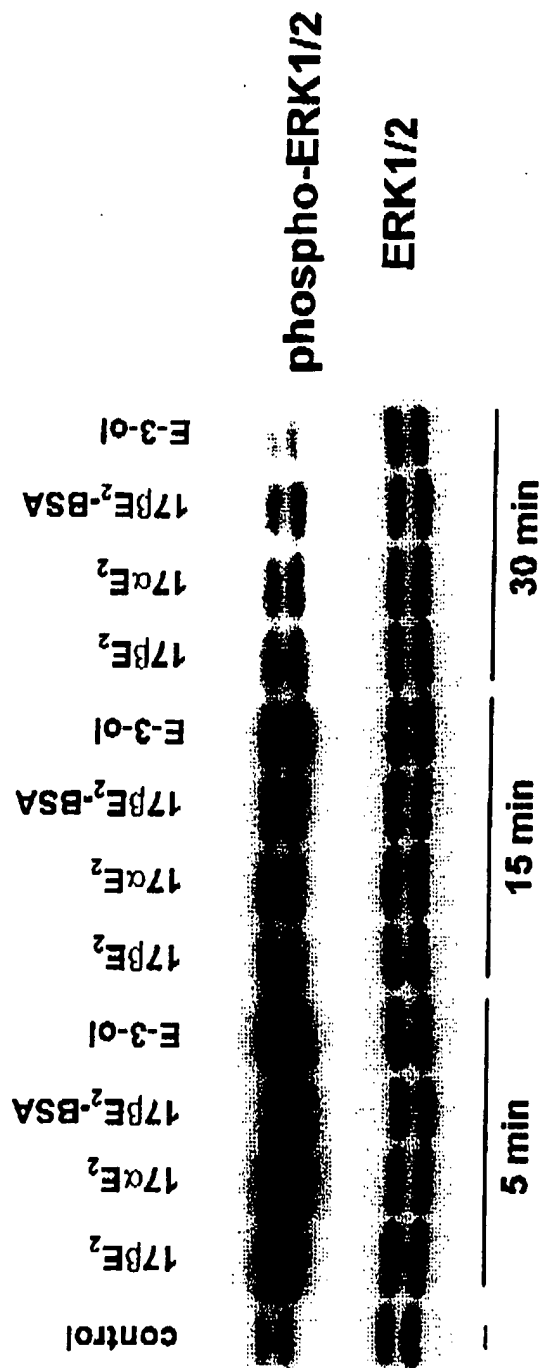


Figure 8: Activation of Extracellular Signal Regulated Kinases (ERKs)

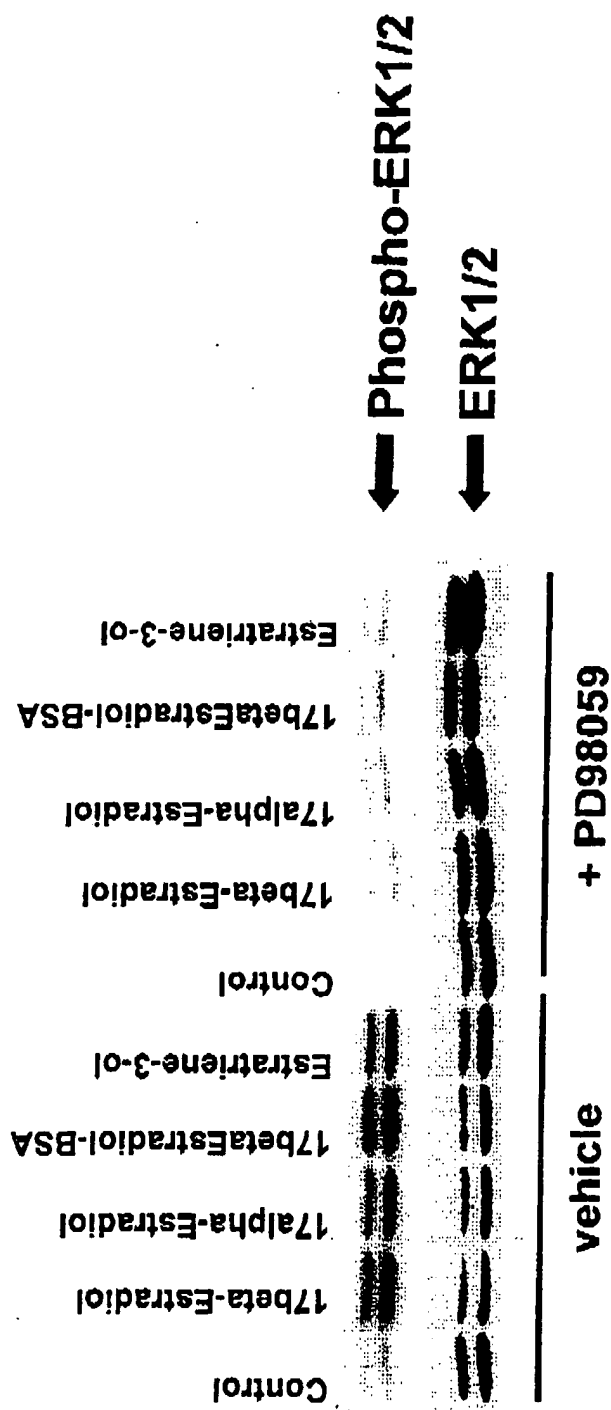


Figure 9: The effect of estrogenic compounds on the activation of ERK1/2 is blocked by a specific inhibitor.

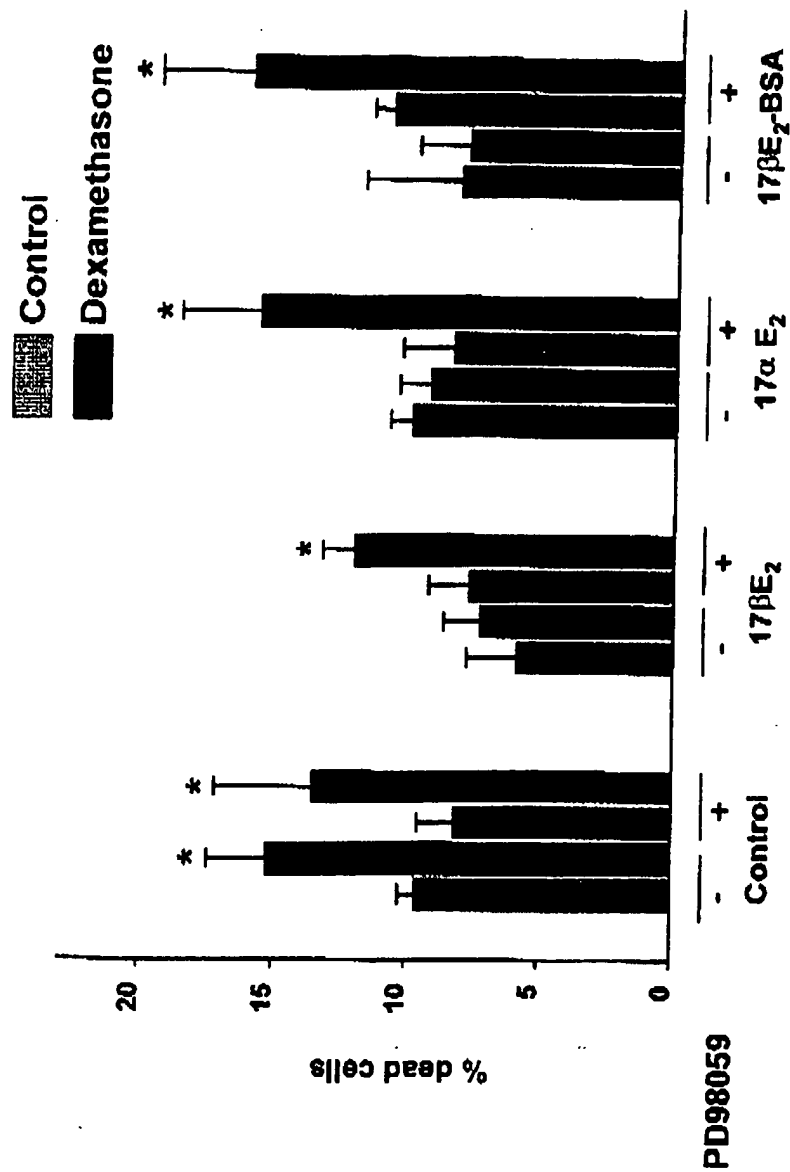


Figure 10: The specific inhibitor of ERK activation abolishes the anti-apoptotic effect of the estrogenic compounds.

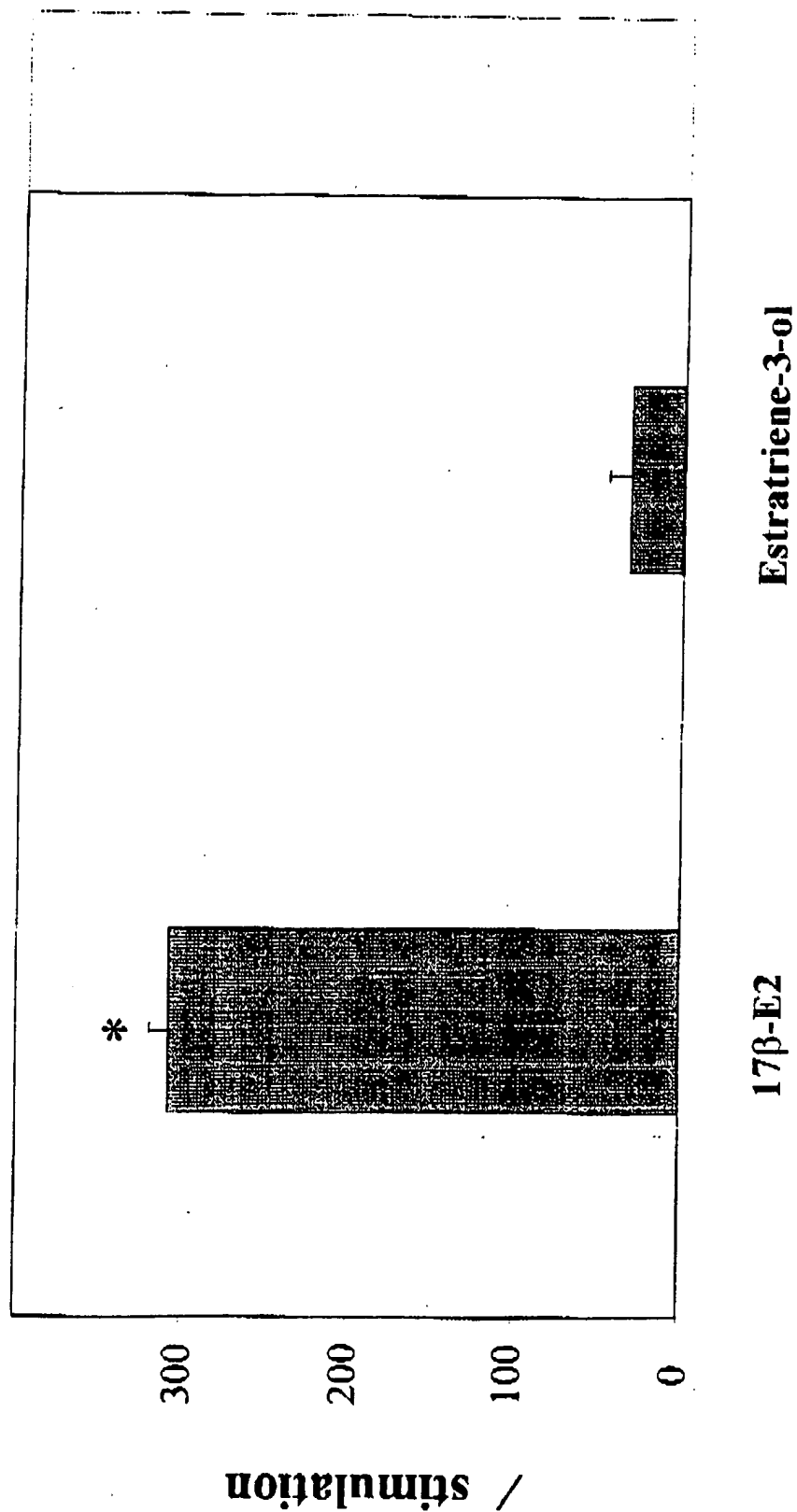
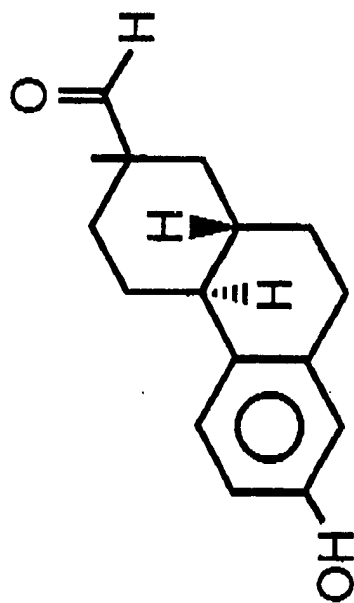
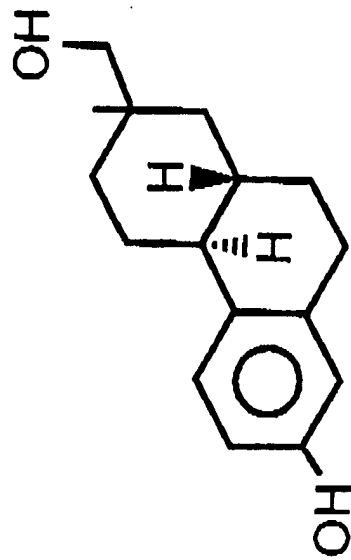


Figure 11 : Unlike 17β estradiol, estratriene-3-ol does not transactivate an estrogen response through ERα.



$C_{16}H_{20}O_2$
MW=244

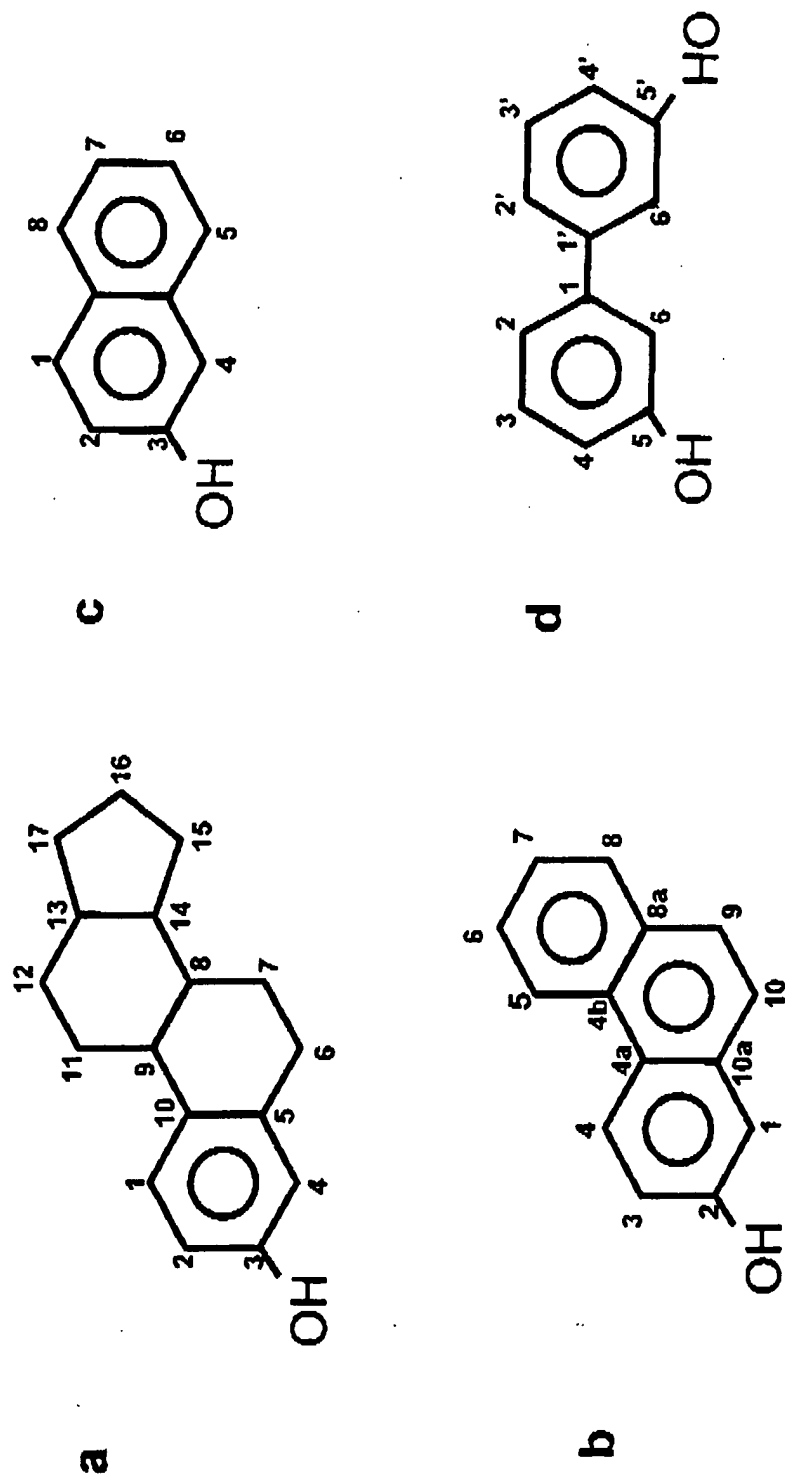
[2S-(2a,4a α ,10a β)]-1,2,3,4,4a,9,10,10a-Octahydro-7-hydroxy-2-methyl-2-phenanthrenecarboxaldehyde



$C_{16}H_{22}O_2$
MW=246

[2S-(2a,4a α ,10a β)]-1,2,3,4,4a,9,10,10a-Octahydro-7-hydroxy-2-methyl-2-phenanthrenemethanol

Figure 12



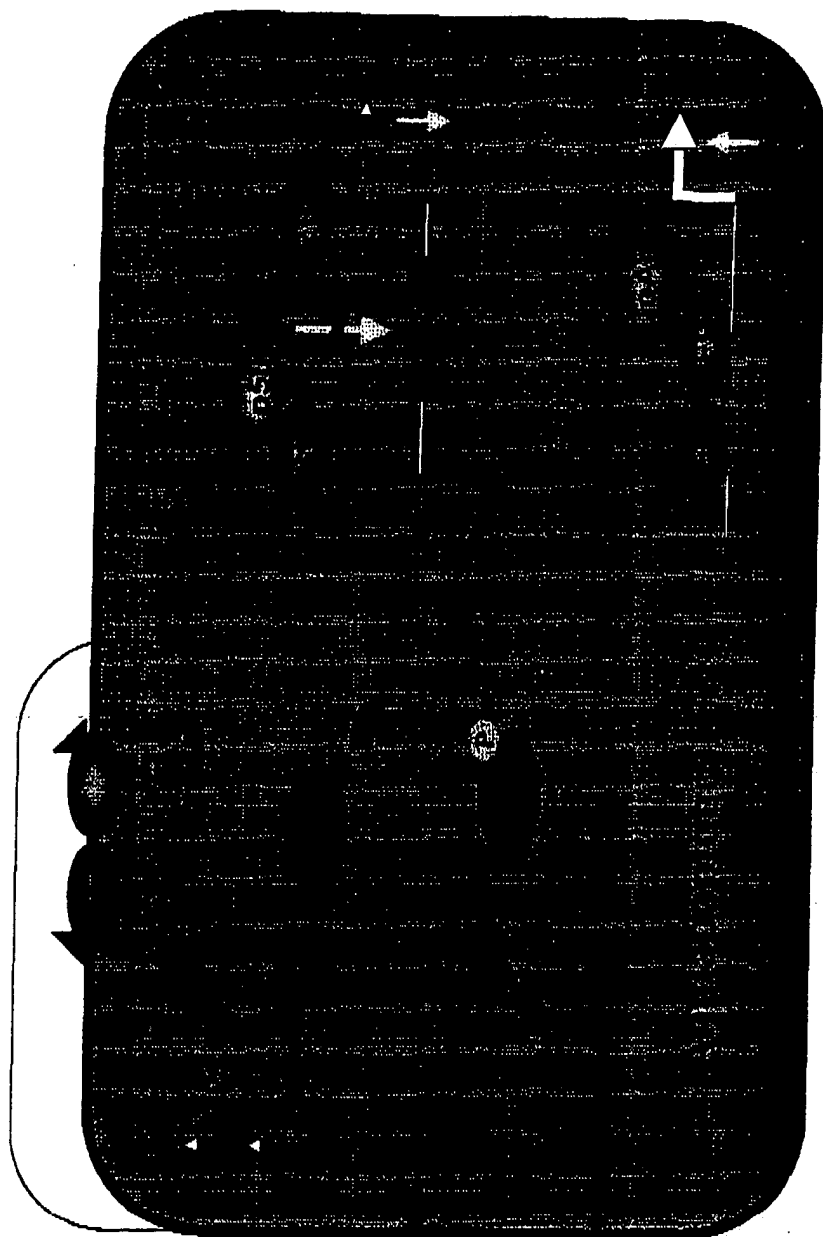


Figure 14: Mechanisms of Estrogen Receptor Action

Formation occurs only on sites of previous osteoclastic bone resorption.

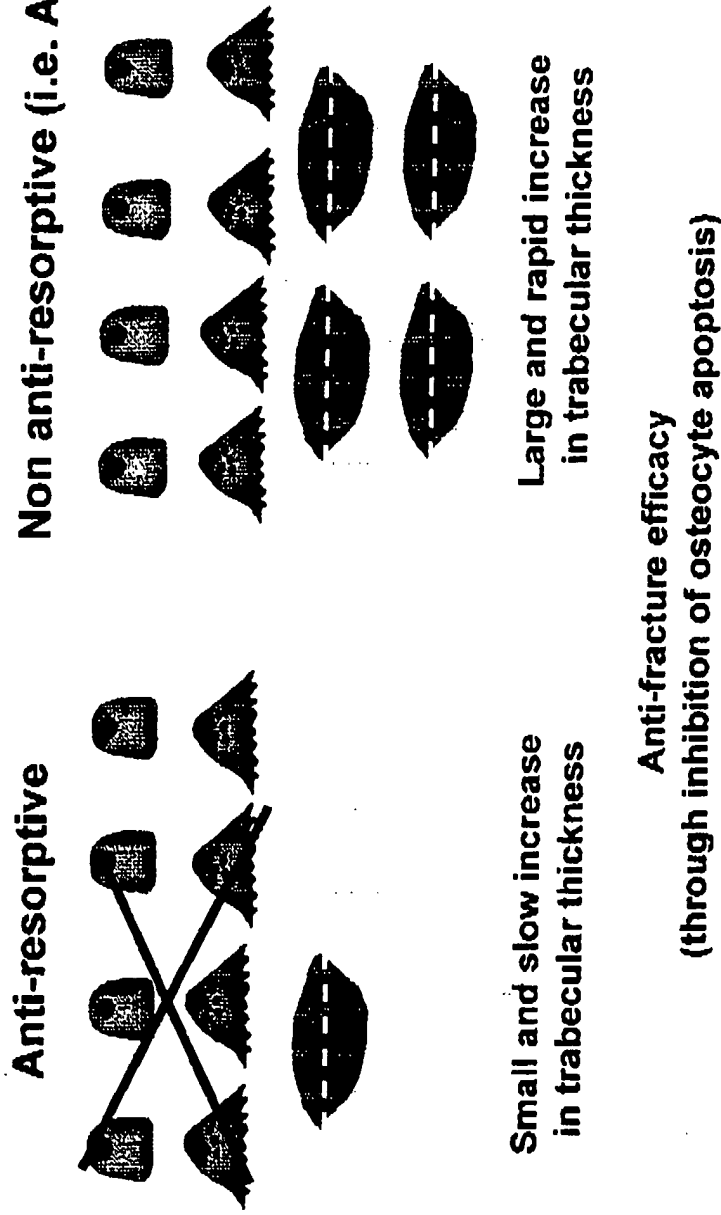


Figure 15: Implications of the effects of anti-resorptive vs. non anti-resorptive agents on apoptosis

R AND/OR R' SUBSTITUTION	
	STRUCTURE
HYDROXY-	$-OH$
METHYL-	$-CH_3$
METHYL ESTER	$-OCH_3$
ACETYL-	$O-\underset{\text{CH}_3}{\underset{ }{C}}-$
ETHYL ESTER	$O-CH_2-CH_3$
3, 3, 10, 10-DIMETHYL-	$\begin{matrix} \diagup OCH_3 \\ \diagdown OCH_3 \end{matrix}$
ETHYNYL-	$\begin{matrix} \diagup C \equiv CH \\ \diagdown \end{matrix}$
BENZOYL-	$O-\underset{\text{C}_6\text{H}_5}{\underset{ }{C}}-$
BENZYL ESTER	$OCH_2-\text{C}_6\text{H}_5$
GLUCURONIC	$C_6H_8O_6$
SULFATE SODIUM :	OSO_3Na
CYCLOHEXYL-	$=$
VALERYL-	$-C_5H_9O$
CYCLOPENTYLPROPYL-	$-O-\underset{\text{C}}{\underset{ }{C}}-(CH_2)_2-\text{Cyclopentyl}$
PROPYL-	$-O-\underset{\text{C}}{\underset{ }{C}}-(CH_2)_2$
HEMISUCCINYL-	$-C_4H_4O_3$
PALMITIC	$-C_{16}H_{32}O_2$

Figure 16A

R₁ AND/OR R₂ SUBSTITUTIONS

STRUCTURE

SODIUM PHOSPHATE



ENANTHATE



GLUCURONIDE SODIUM SALT



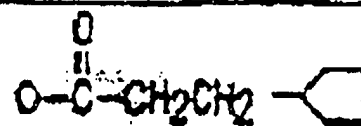
STEARATE



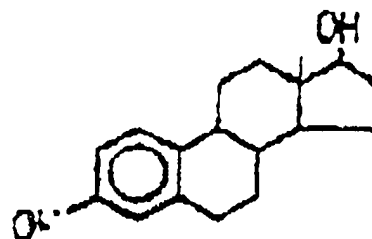
TRIETHYLAMMONIUM SALT



CYCLOPENTYL



17β ESTER



17α ESTER

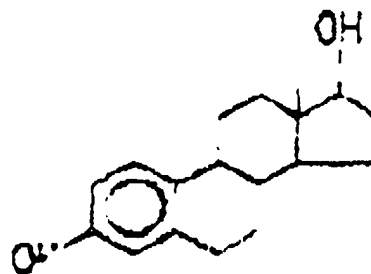


Figure 16B

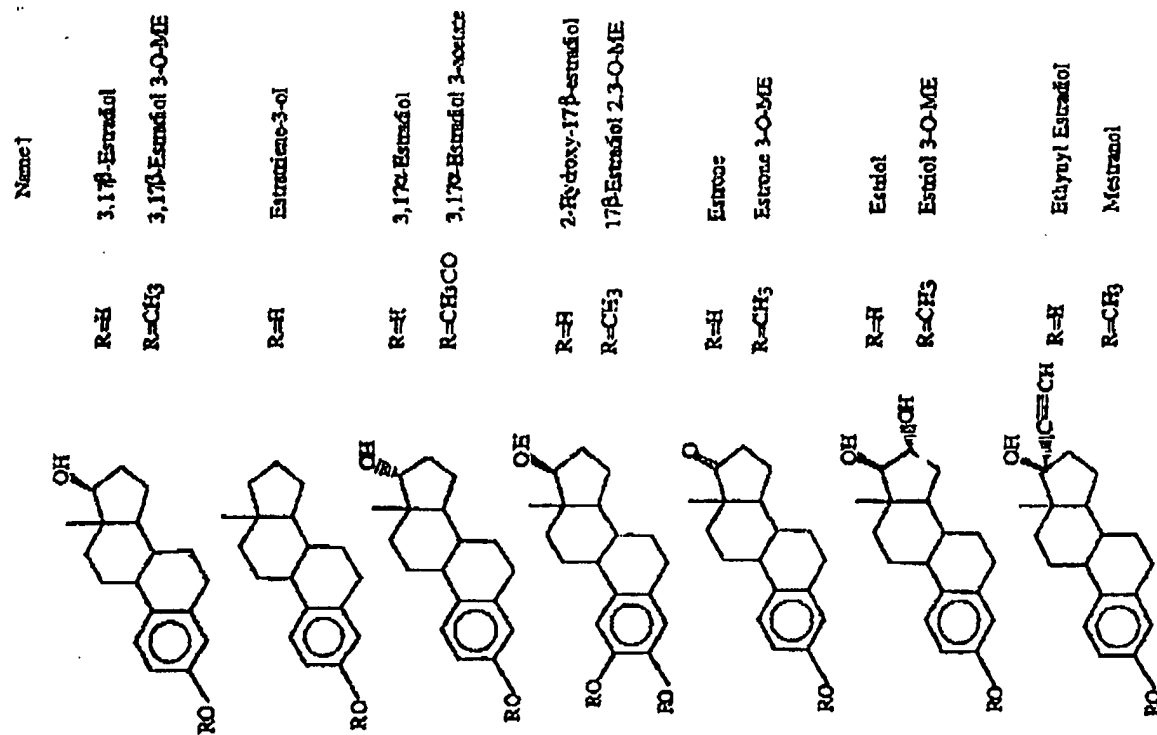


Figure 17

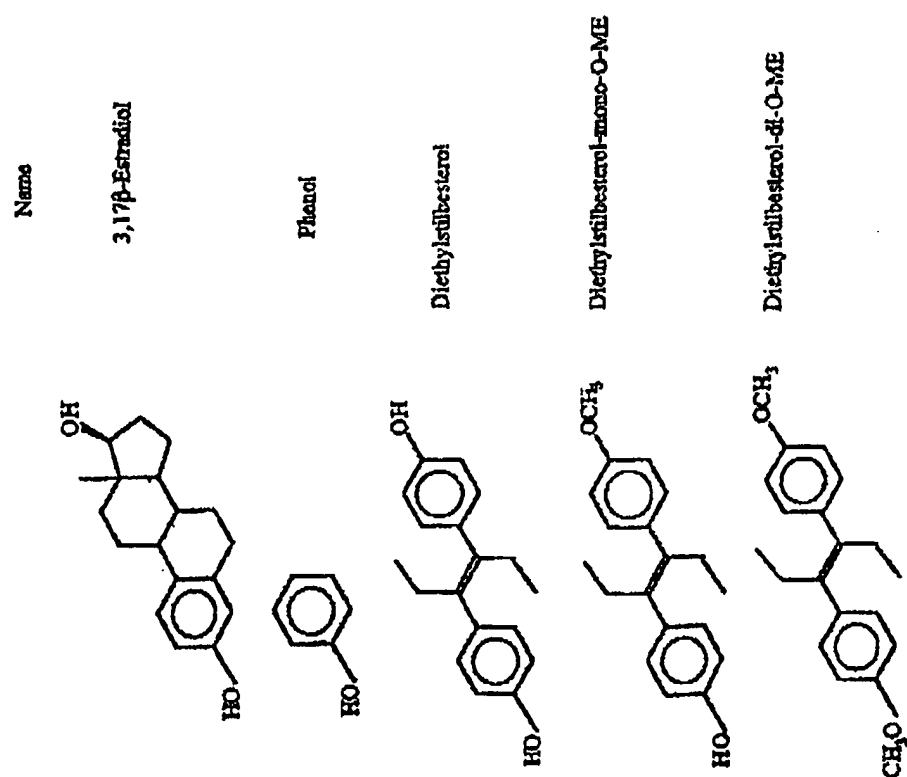


Figure 18

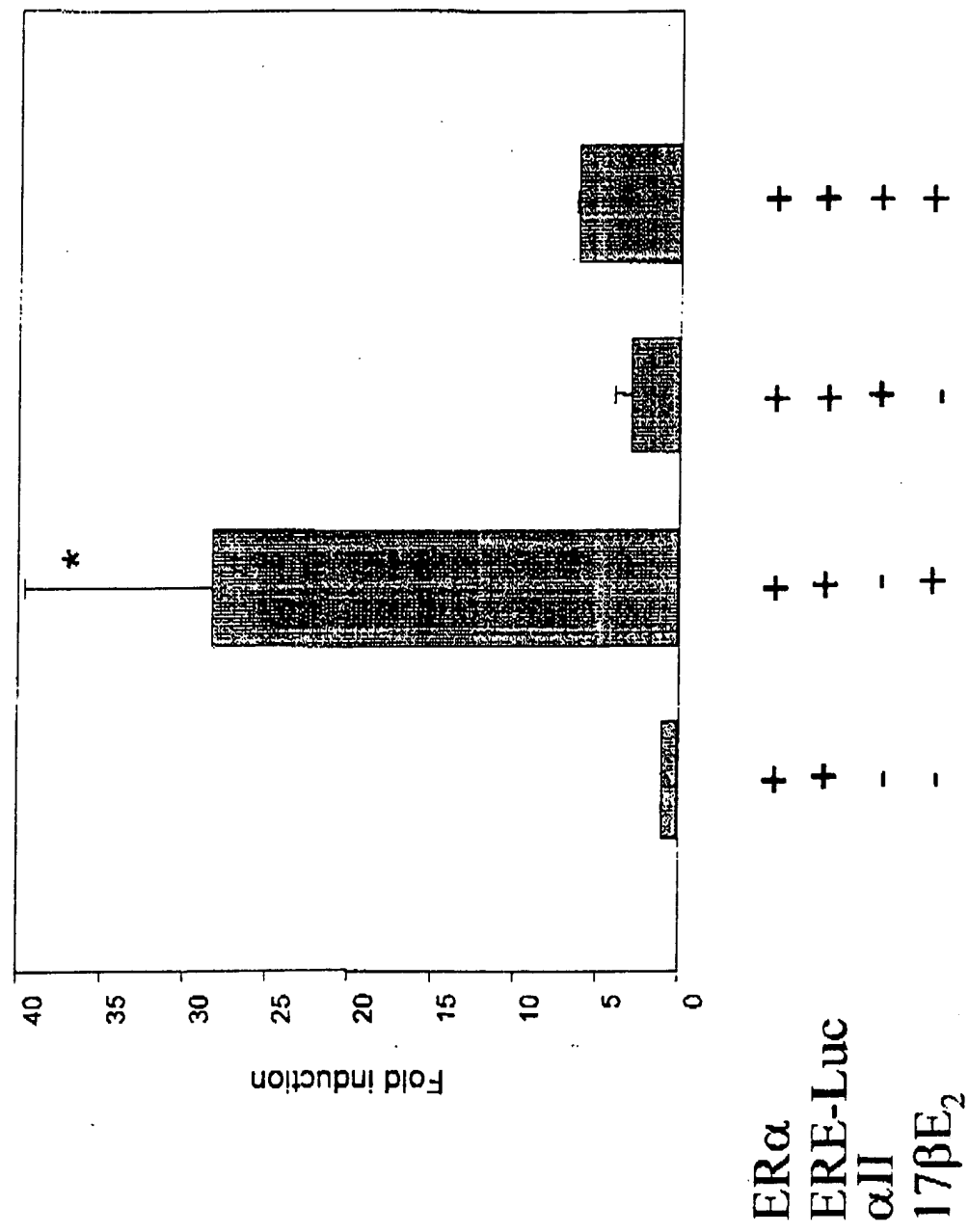


Figure 19: Effect of the all peptide on the 17βE₂-induced ERE activity in 293 cells

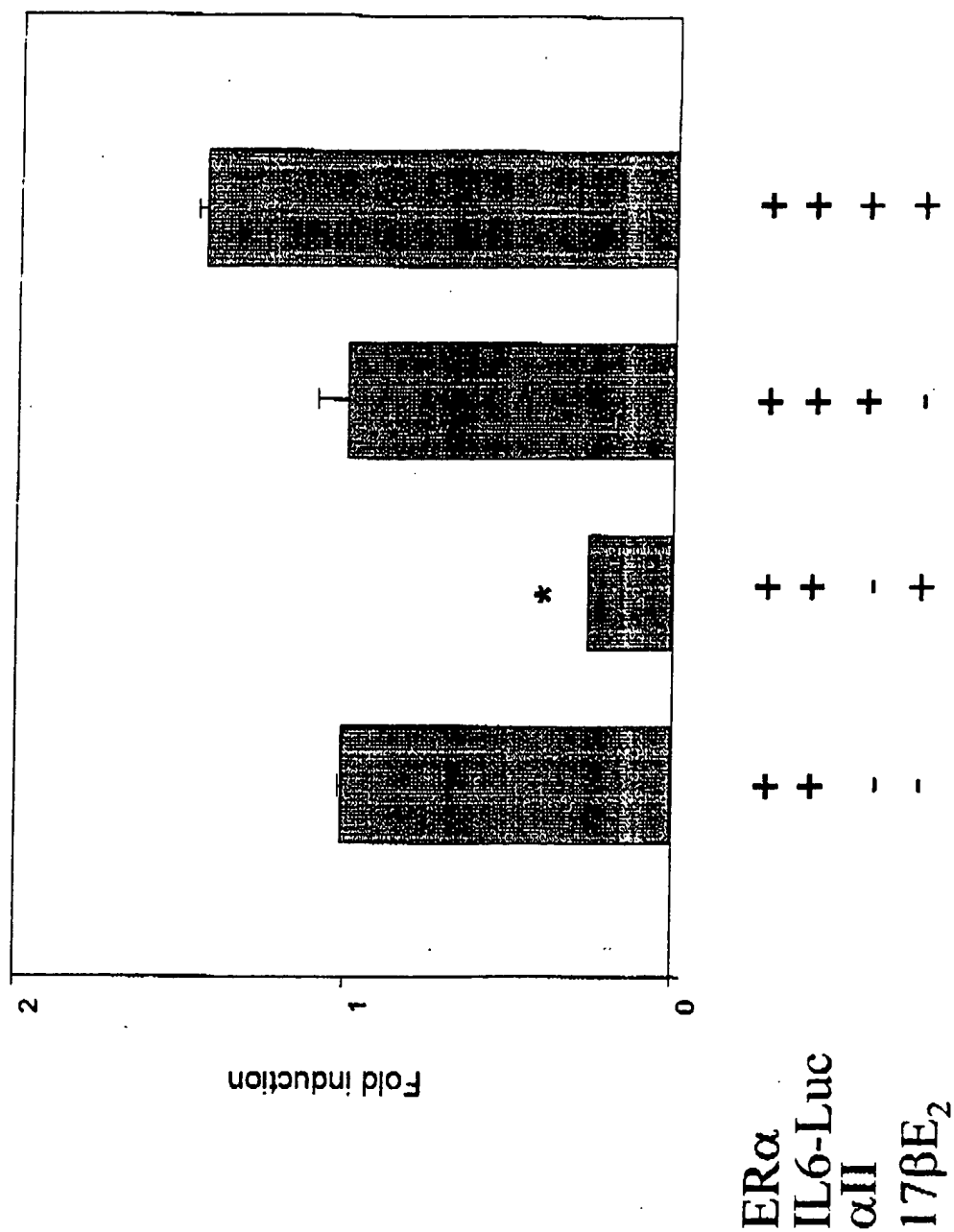


Figure 20: Effect of the all peptide on the 17βE₂-induced inhibition of IL-6 activity in 293 cells

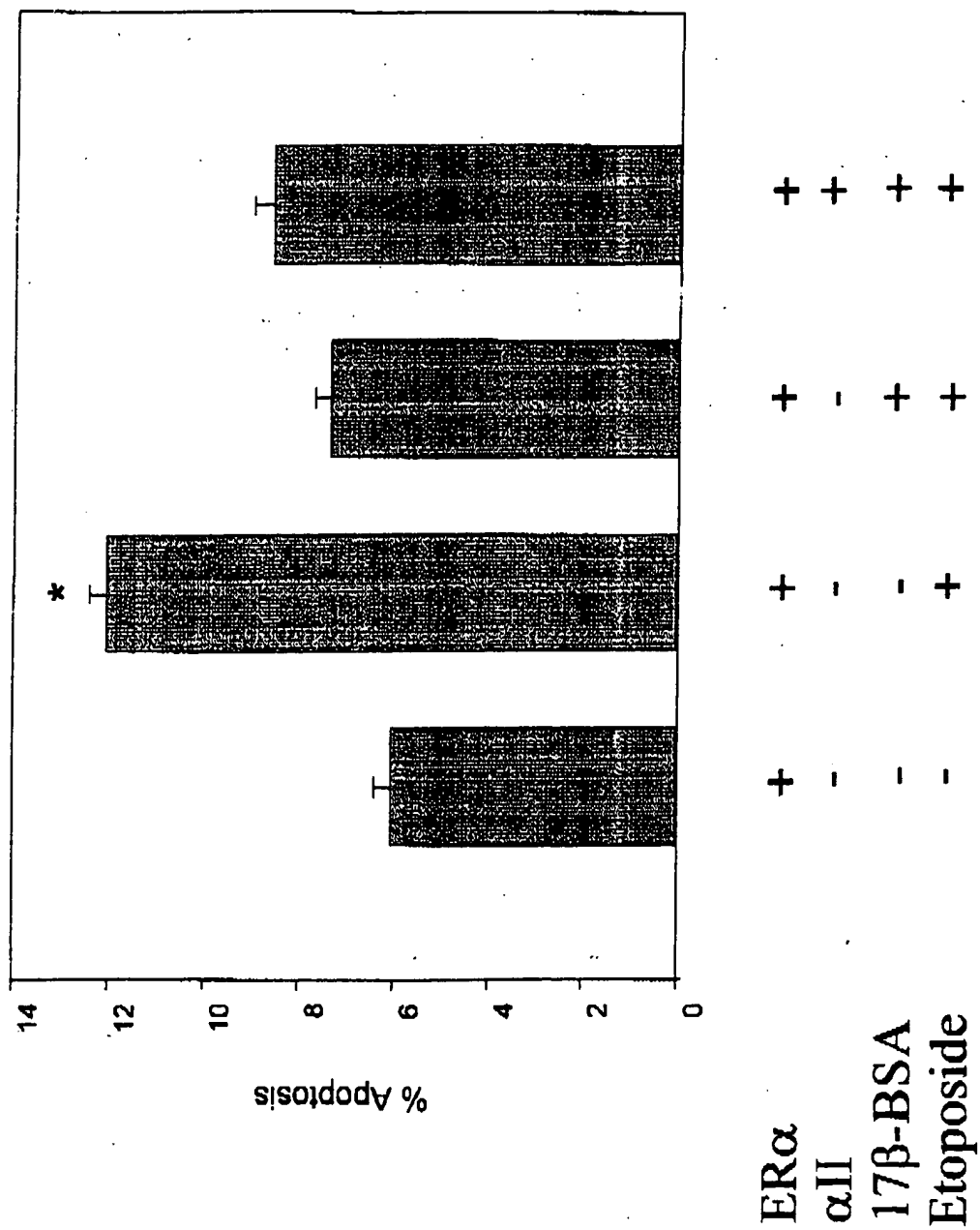


Figure 21: Effect of the all peptide on the Etoposide-induced apoptosis of 17b-BSA-activated 293 cells